Internal dissipation and self-excited ocillations in rotating machinery: internal friction vs. internal viscous damping

Hartmut Hetzler, Felix Boy

Internal dissipation and self-excited ocillations in rotating machinery: internal friction vs. internal viscous damping

Hartmut Hetzler[1]*, Felix Boy[1]

ISROMAC 2017

International Symposium on Transport Phenomena and Dynamics of Rotating Machinery

Maui, Hawaii

December 16-21, 2017

Abstract
Destabilization due to co-rotating internal viscous damping is a very well known phenomenon. However, most practical applications in engineering do rather exhibit frictional damping (stemming from joints, etc.) instead of velocity proportional dissipation. This contribution aims on investigating the basic effects of internal damping due to co-rotaing frictional dissipation and the interaction with external damping. It is found that adding internal friction damping alters the dynamical behavior significantly: the threshold rotation speed depending on D_e/D_i known from the linear problem is replaced by self-excited vibrations due to the frictional damping which occur between the resonance speed and the linear threshold speed and which grow hyperbolically as the linear threshold speed is approached. However, the result of the linear analysis is still meaningful since it marks the maximum speed until which finite amplitudes are to be expected.

Keywords
Joint damping — Friction

[1]*Department of Mechanical Engineering, University of Kassel, Kassel, Germany*
***Corresponding author**: hetzler@uni-kassel.de

INTRODUCTION

Among dynamical stability problems in general, self-excited vibrations are major issues in rotordynamical applications which may lead to severe problems in acoustics or even limit operational regimes and lifetime [1],[2],[3],[4]. Apart from self-excitation due to rotor-fluid interaction in fluid-film bearings whip [2],[1],[5] or annular sealings [3], [6], vibrations stemming from co-rotating dissipation (so called "internal damping") are a common source for self-excitated vibrations [6],[7],[3],[8].

Apart from material damping, co-rotating dissipation usually stems from shrink fits, joint connections or inter-laminar friction in rotor-stacks of electric machines. Historically, it was this latter application which led to the discovery of the destabilizing effect of internal damping [9],[10],[11]. In the context of this contribution it is interesting to note that the first contributions on this dynamical problem already used the term "internal friction" – however, since then almost all investigations had been restricted to the influence of various types of linear or non-linear viscous damping and accordingly the wording changed from "internal friction" to "internal damping". Reviewing the literature revealed only very few studies on the effect of co-rotating dissipation due to dry friction. Most of them focussed on forced vibrations [12],[13] while the influence on stability and self-excitation has only be touched superficially [14].

Recent experiments emphasize that an appropriate modelling of the dissipation in rotor stacks of electric machinery demands for modelling approaches involving dry friction [15],[16].

Not only for rotordynamical instabilities, but even for stability theory in general the impact of dry friction has not yet been investigated into detail. While the literature on dynamical effects of joints in the context of forced vibrations is quite rich (cf. [17],[18], [19],[20] for instance), over a long time only very few publications had been devoted to the impact of dry friction on the bifurcation behavior and it only recently began to attract more attention [21],[22],[23],[24],[25]. However, the significant impact of Coulomb-type damping to stability problems has already been proved experimentally ([26], [22] for instance).

This contribution aims on investigating the influence of co-rotating dissipation due to dry friction, i.e. internal frictional damping, on stabiliy and bifurcation of a generic elastic rotor. To this end, the classical model problem [6] is extended by adding rotor-fixed Coulomb elements. Subsequently, this model problem is investigated with respected to stationary steady state solutions where the Coulomb elements stick, as well as periodic steady state solutions.

1. MODEL

1.1 Equations of motion

The classical model problem to investigate the basic mechanism of self-excitation due internal damping and the influence of external damping is a Jeffcott rotor (Laval rotor) consisting of a massless shaft (lateral stiffness c) in rigid bearings, to which a rigid disk (mass m) is symmetrically mounted (cf. fig.1) and rotates about a principle axis of inertia. Due to the aligned mounting dynamic unbalance due to gyroscopic effects will not occur. Moreover it is assumed that the mounting point M of the disk coincides with the center of mass G: hence, excitation due to static unbalance will not occur, neither. The shaft rotates with a constant angular velocity Ω. The influence of gravity is not taken into account.

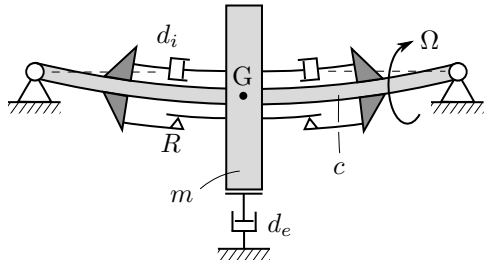

Figure 1. Jeffcott rotor model with internal friction and internal viscous damping.

In addition to the conservative forces, the rotor is subjected to viscous *external damping* (coefficient of viscous damping d_e) due to motion with respect to the environment as well as *internal dissipation* due to relative motion with respect to the rotor. For the classical model this latter internal dissipation is modelled as co-rotating linear-viscous damping (coefficient d_i). For the present study, the classical model is extended by adding co-rotating Coulomb elements (amplitude R of the friction force) to the internal damping.

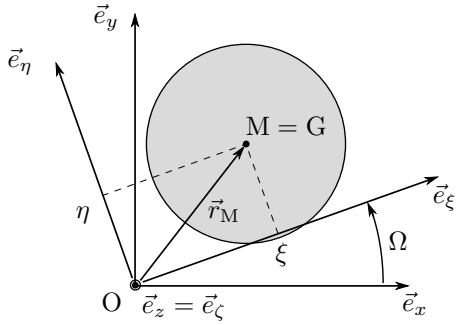

Figure 2. Kinematics with inertial frame $\mathcal{I}$ and co-rotating frame $\mathcal{R}$.

For the analysis two frames of reference are introduced (cf.figure 2): one inertial frame $\mathcal{I} = \{\mathrm{O}, [\vec{e}_x, \vec{e}_y, \vec{e}_z]\}$ and a co-rotating relative frame $\mathcal{R} = \{\mathrm{O}, [\vec{e}_\xi, \vec{e}_\eta, \vec{e}_\zeta]\}$ rotating with the shaft. In the following, for time derivatives leading supercripts will denote the observer system with respect to which the derivative will be calculated: thus, ${}^{\mathcal{R}}\frac{\mathrm{d}}{\mathrm{d}t}()$ will denote time derivatives with respect to an observer moving with system $\mathcal{R}$.

Both internal friction and internal viscous damping depend on the relative velocity $\vec{v}_\mathrm{rel} = {}^{\mathcal{R}}\frac{\mathrm{d}}{\mathrm{d}t}(\vec{r}_M)$ of the mounting point M with respect to the co-rotating frame of reference $\mathcal{R}$. Using Euler's differentiation formula one finds the velocity relation

$$\dot{\vec{r}}_\mathrm{M} = {}^{\mathcal{I}}\frac{\mathrm{d}\vec{r}_\mathrm{M}}{\mathrm{d}t} = \vec{v}_\mathrm{rel} + \vec{\Omega} \times \vec{r}_\mathrm{M},$$

where $\vec{\Omega} = \Omega\vec{e}_z$ is the vector of the angular velocity. With this, the *internal viscous damping* force can be written as

$$\vec{F}_{d_i} = -d_i\vec{v}_\mathrm{rel} = -d_i\left(\dot{\vec{r}}_\mathrm{M} - \vec{\Omega} \times \vec{r}_\mathrm{M}\right).$$

The *internal friction* force is modeled using Coulomb's friction law. Accounting for sticking and sliding, the force reads

$$\vec{F}_r = \begin{cases} -R\frac{\vec{v}_\mathrm{rel}}{||\vec{v}_\mathrm{rel}||} & , \quad ||\vec{v}_\mathrm{rel}|| \neq 0 \\ \vec{F}_\mathrm{s} & , \, ||\vec{F}_r|| < R \wedge ||\vec{v}_\mathrm{rel}|| = 0 \end{cases} \tag{1}$$

where the first line represents the sliding friction force and $\vec{F}_\mathrm{s}$ is the a priori unknown reaction force while sticking. The set $\mathcal{F} \ni \vec{F}_\mathrm{s}$ of admissible stiction forces represents a closed circle of radius R within the (F_ξ, F_η)- plane (cf. figure 3).

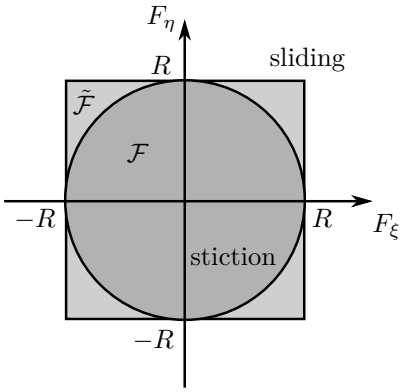

Figure 3. Set $\mathcal{F}$ of admissible stiction forces and the approximation set $\tilde{\mathcal{F}}$ in the (F_ξ, F_η)- plane.

In order to find closed form approximations of stationary solutions the friction law (1) is simplified to

$$\vec{F}_r \approx \tilde{\vec{F}}_r \in -R\,\left(\mathrm{Sign}(\dot{\xi})\vec{e}_\xi + \mathrm{Sign}(\dot{\eta})\vec{e}_\eta\right)$$

for the following investigations. Formally, this can be interpreted as a first order polyhedral approximation of the friction cone. Here, the set-valued Sign function defined as

$$\mathrm{Sign}(x) = \begin{cases} \mathrm{sign}(x) & , |x| \neq 0 \\ [-1, 1] & , |x| = 0 \end{cases}$$

is used [27].

This simplified friction law implies a rectangular set $\tilde{\mathcal{F}}$ of stiction in the (F_ξ, F_η)- plane, as it is also shown in figure 3. From the graph it can be seen that this approximation set is slightly larger than the original one and contains it, i.e. $\mathcal{F} \subset \tilde{\mathcal{F}}$. Thus, it will describe the friction accurately for most cases and will overestimated it only for some cases: the effect and the interpretation of this simplification will be discussed within the results section.

For the forces mentioned above, the equations of motion become

$$m\ddot{\vec{r}}_{\mathrm{M}} + d_e\dot{\vec{r}}_{\mathrm{M}} + d_i\left(\dot{\vec{r}}_{\mathrm{M}} - \vec{\Omega}\times\vec{r}_{\mathrm{M}}\right) + c\vec{r}_{\mathrm{M}} = \tilde{F}_r.$$

Introducing the nondimensional time $\tau = \omega_0 t$ with $\omega_0^2 = \frac{c}{m}$ they can be rewritten as

$$\vec{r}_{\mathrm{M}}^{\,\prime\prime} + 2(D_e + D_i)\vec{r}_{\mathrm{M}}^{\,\prime} + \vec{r}_{\mathrm{M}} - 2D_i\vec{\Omega}\times\vec{r}_{\mathrm{M}} = \frac{\tilde{F}_r}{c},$$

where $D_e = \frac{d_e}{2m\omega_0}$, $D_i = \frac{d_i}{2m\omega_0}$ and $()' = \mathrm{d}/\mathrm{d}\tau()$ is the derivative with respect to the dimensionless time τ. Introducing $\rho = \frac{R}{c}$ and refering to the co-rotating frame of reference $\mathcal{R}$, the equations of motion read

$$\begin{aligned}\begin{bmatrix}\xi''\\ \eta''\end{bmatrix} + \begin{bmatrix}2(D_e+D_i) & -2\nu\\ 2\nu & 2(D_e+D_i)\end{bmatrix}\begin{bmatrix}\xi'\\ \eta'\end{bmatrix}\\ + \begin{bmatrix}1-\nu^2 & -2D_e\nu\\ 2D_e\nu & 1-\nu^2\end{bmatrix}\begin{bmatrix}\xi\\ \eta\end{bmatrix}\\ \in -\rho\begin{bmatrix}\mathrm{Sign}(\xi')\\ \mathrm{Sign}(\eta')\end{bmatrix},\end{aligned} \tag{2}$$

where $\nu = \frac{\Omega}{\omega_0}$ is the normalized rotational speed and ξ, η are the coordinates of $\vec{r}_M$ with respect to the co-rotating frame.

Due to the set-valued character of the right-hand side these equations allow for two kinds of solutions: equilibria (sticking) at the one hand side, and sliding motions on the other hand.

1.2 Sticking friction elements: Equilibria in the co-rotating frame

If the co-rotating friction damper elements stick permantly the relative motion vanishes, i.e. $\xi'' = \xi' = \eta'' = \eta' = 0$ must hold: this corresponds to an equilibrium solution in the co-rotating frame $\mathcal{R}$. Since sticking may occur not only at one position but within an interval of positions, the equilibrium solutions belongs to a set, i.e.

$$\begin{bmatrix}\xi_0\\ \eta_0\end{bmatrix} \in \quad \mathcal{E} = -\rho\begin{bmatrix}1-\nu^2 & -2D_e\nu\\ 2D_e\nu & 1-\nu^2\end{bmatrix}^{-1}\begin{bmatrix}\mathrm{Sign}(0)\\ \mathrm{Sign}(0)\end{bmatrix}.$$

Since this is an affine mapping of the convex and polygonal set $\mathrm{Sign}(\mathbf{0})$, the sticking set $\mathcal{E}$ will also be a convex polygone.

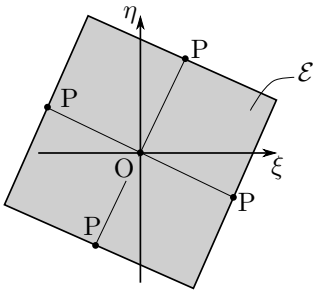

Figure 4. Set of equilibrium positions (ξ_0, η_0) in the (ξ, η) -plane.

Moreover, since the mapping is given by an orthogonal matrix, it will only comprise scaling and rotation but without any distorting. Thus, depending on the mapping parameters ν and D_e and the friction parameter ρ, the stiction set $\mathcal{E}$ will be scaled and rotated square: figure 4 shows an example for $(\nu, D_e) = (0.8, 0.1)$. In order to visualise the influence of the parameters $(\nu,\ D_e,\ \varrho)$ on the size of $\mathcal{E}$ figure 5 shows the relative length $\overline{\mathrm{OP}}/\varrho$ versus the rotational speed ν for different values of D_e. Please note that the size of $\mathcal{E}$ is the same shape as the magnification factor of a forced 1DoF-oscillator and that the equilibrium solutions refer to the rotor-fixed frame of reference. Thus, an observer from the inertial frame $\mathcal{I}$ will observe oscillations with a constant amplitude $A_0 \leq \sqrt{2}\,\overline{\mathrm{OP}}$ and the frequency ν of the rotor.

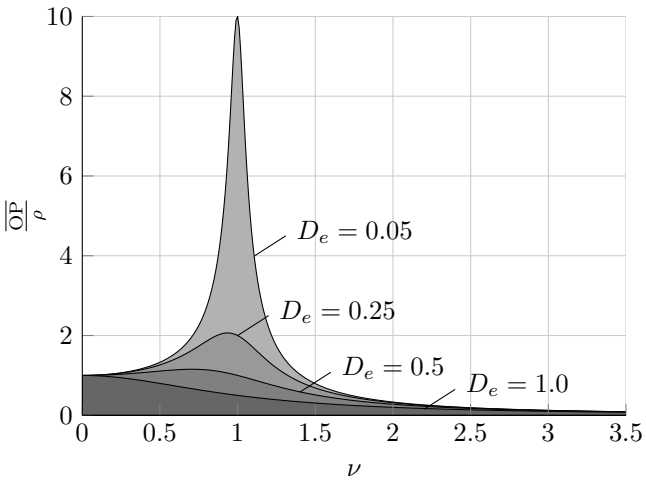

Figure 5. Width $\overline{\mathrm{OP}}$ of the stiction set $\mathcal{E}$ depending on ν and D_e.

1.3 Sliding frictional elements: periodic solutions in the co-rotating frame

Numerical simulations indicate, that there also exists a stable limit cycle for $\nu > 1$ if internal friction is present. Here, Galerkin's method will be used to find an approximation to this stationary solution. In the sense of a truncated first order Fourier-series approximations of

stationary periodic solutions may be searched using

$$\xi \approx \bar{\xi} = A_\xi \cos(\omega\tau), \tag{3}$$
$$\eta \approx \bar{\eta} = A_\eta \cos(\omega\tau + \psi), \tag{4}$$

where $A_\xi, A_\eta > 0$; $\omega, \psi \in \mathbb{R}$. Here, the formula for the first coordinate does not contain a phase shift since for autonomous systems this phase angle may always be eliminated by shifting the time datum.

Introducing (3), (4) into the equation of motion (2) yields the residuum $r = r(A_\xi, A_\eta, \omega, \psi)$. Then, Galerkin projection over one oscillation period using the ansatz functions as weighting functions yields

$$A_\xi \left(1 - (\omega^2 + \nu^2)\right) + 2A_\eta \left(\sin\psi\omega - D_e \cos\psi\right)\nu = 0 \tag{5}$$
$$A_\eta \left(1 - (\omega^2 + \nu^2)\right) + 2A_\xi \left(\sin\psi\omega + D_e \cos\psi\right)\nu = 0 \tag{6}$$

$$-A_\xi \left(D_e + D_i\right)\omega + A_\eta \left(+\cos\psi\omega + D_e \sin\psi\right)\nu - \mathrm{sign}(\omega)\frac{2\rho}{\pi} = 0 \tag{7}$$

$$-A_\eta \left(D_e + D_i\right) + A_\xi \left(-\cos\psi\omega + D_e \sin\psi\right)\nu - \mathrm{sign}(\omega)\frac{2\rho}{\pi} = 0 \tag{8}$$

Equations (5)-(8) show some type of pairwise anti-symmetry: from this one may observe that

$$A_\xi = A_\eta =: A \tag{9}$$
$$\cos\psi = 0 \rightarrow \sin\psi = \pm 1 \tag{10}$$
$$\rightarrow \psi_1 = +\pi/2\,,\ \psi_2 = -\pi/2 \tag{11}$$

are obvious solutions. The phase shift implies circular orbits, which is a reasonable since with regard to the symmtry of the system. Using these first results, two more equations for the unknowns A and ω are obtained

$$A[(D_e + D_i)\omega - D_e \nu \sin\psi] = -\mathrm{sign}(\omega)\frac{2\rho}{\pi} \tag{12}$$
$$\omega^2 - 2(\nu \sin\psi)\,\omega - (1 - \nu^2) = 0. \tag{13}$$

Solving for A and ω yields four solutions. However, since $A > 0$ had been assumed only two admissible solutions remain, having the same amplitude A but opposite angular velocity and sign of phase angle, i.e.

$$1)\ (A, \omega, \psi = \pi/2) \qquad 2)\ (A, -\omega, \psi = -\pi/2).$$

The corresponding approximate solutions read

$$1)\ \xi = A\cos\omega\tau \qquad 2)\ \xi = A\cos\omega\tau$$
$$\eta = A\cos(\omega\tau + \pi/2) \qquad \eta = A\cos(\omega\tau - \pi/2)$$
$$= -A\sin\omega t \qquad = A\sin\omega t.$$

Further analysing these two analytical results reveals that the solutions 1) and 2) both describe the same backward whirling motion within the co-rotating frame, as shown in figure 6.

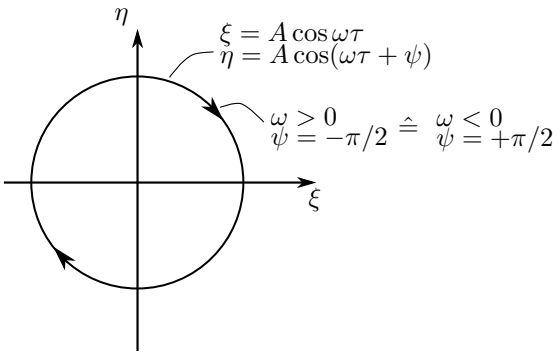

Figure 6. Backward whirl of stationary periodic solutions with respect to the co-rotating frame.

In the following, solution 2) for $\psi = -\frac{\pi}{2}$ will be referenced since the sign of ω directly expresses the backward whirling motion in an obvious way. For this, amplitude, frequency and range of validity of the limit cycle is given by

$$A_{\mathrm{LC}} = \frac{2\rho}{\pi}\frac{1}{D_e + D_i(1-\nu)} \tag{14}$$
$$\omega_{\mathrm{LC}} = 1 - \nu, \quad 1 < \nu < 1 + \frac{D_e}{D_i}. \tag{15}$$

Please note that this is the angular frequency of motions with respect to the co-rotating frame. For an inertial observer, the co-rotating back-ward whirl will compensate the rotational speed of the rotor and oscillations with the constant angular frequency ${}^{\mathcal{I}}\omega_{\mathrm{LC}} = 1$ will be seen.

2. RESULTS

Within this section, the analytical approximations shall be compared to numerical simulations and analysed from a physical point of view. The discussion starts with a short review of results for internal viscous damping only ($\rho = 0, D_i \neq 0$), known from classical textbooks [6],[3],[4]. Subsequently the system with internal friction only ($\rho > 0, D_i = 0$) is investigated. Finally the interaction between internal friction and internal viscous damping ($\rho > 0, D_i > 0$) is analysed. In addition, the effect of approximating the circular set of equilibria $\mathcal{E}$ by a rectangular shape $\tilde{\mathcal{E}}$ will be addressed.

2.1 The standard model: internal viscous damping only

The classical approach to model internal damping is based on co-rotating linear viscous damping without accounting for dry friction, i.e. $\rho = 0, D_i \neq 0$. In this case, the steady state solution to (2) is the trivial solution $(\xi_0, \eta_0) = (0, 0)$ – thus, the set $\mathcal{E}$ degenerates to a single point. Moreover, it is found that this trivial solution loses its stability at a threshold speed of $\nu_{\mathrm{crit}} = 1 + \frac{D_e}{D_i}$.

This stability threshold is outlined in figure 7. Further analysis shows, that the steady state loses its stability due

to a Hopf-bifurcation: thus, for subcritial speeds perturbations will lead to oscillations with decaying amplitude, while for supercritical speeds the system will oscillate with growing amplitude. Eventually, the growth of amplitude will be limited by some nonlinearity (e.g. nonlinear stiffness or damping for instance): this aspect is not incorporated in the model presented here but is extensively discussed in standard literature on bifurcations.

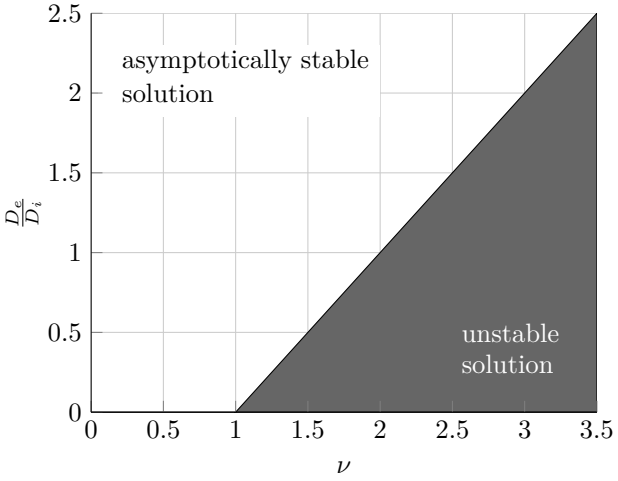

Figure 7. Classic stability chart for internal viscous damping only.

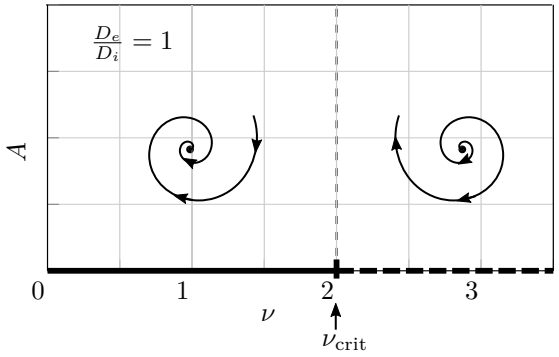

Figure 8. Bifurcation diagramm for the classical model only incorporating viscous damping forces.

2.2 Internal friction only

For the case of viscous external damping and purely frictional internal dissipation – i.e. vanishing of the viscous part of the internal damping – equation (14) for stationary amplitudes simplifies to

$$A_{\text{LC}}\Big|_{D_i=0} = \frac{2}{\pi}\frac{\rho}{D_e} \quad , \quad \forall \nu \geq 1. \tag{16}$$

Obviously, beyond the critical speed $\nu = 1$ self-excited vibrations of finite amplitude will occur.

Figure 9 shows corresponding limit cycle amplitudes versus the rotational speed ν for the example $D_e = 0.1, D_i = 0, r = 0.05$. The analytical prediction $A_{\text{LC}}\big|_{D_i=0}$ for limit cycle amplitudes is indicated by a solid line and is compared to results obtained from a numerical time simulations which is marked by stars. The corresponding limit cycle frequency ω_{LC} observed from the co-rotating frame $\mathcal{R}$ is shown in figure 10. The dark grey region outlines the set of co-rotating equilibria $\mathcal{E}$ where the frictional elements stick.

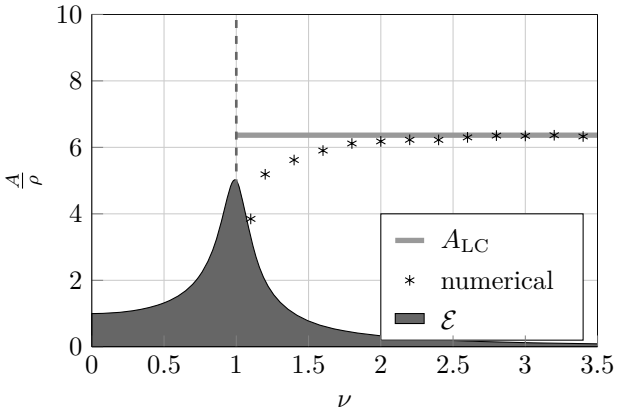

Figure 9. Equilibrium set, analytical approximation an numerical simulations results of the limit cycles vs. ν.

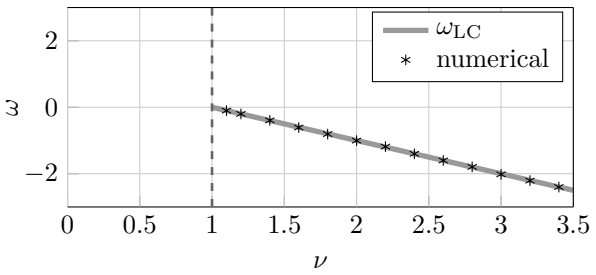

Figure 10. Limit cycle oscillation frequency ω_{LC} vs. rotor speed ν.

It is found, that the analytical prediction $A_{\text{LC}}\big|_{D_i=0}$ for the stationary limit-cycle amplitudes gives very accurate results, apart from the region immediately after the bifurcation at $\nu = 1$. This is due to the fact that close to the bifurcation point the limit cycle orbits are not circular and thus the chosen Galerkin ansatz may only yield rough approximations (cf. fig. 11). Further numerical simulations indicate, that this is related to the chosen polygonal approximation of the friction characteristic (cf. 3) which overestimates the friction for some kinematic constellations. However, the analytical approximation is very accurate in most cases and always yields an upper limit for the model discussed here.

Concerning dynamics it is found that for subcritical speeds $\nu < 1$ the equilibrium set $\mathcal{E}$ is attractively stable: any inital condition will converge to this set and settle down to a point in $\mathcal{E}$. Since the notion of "equi-

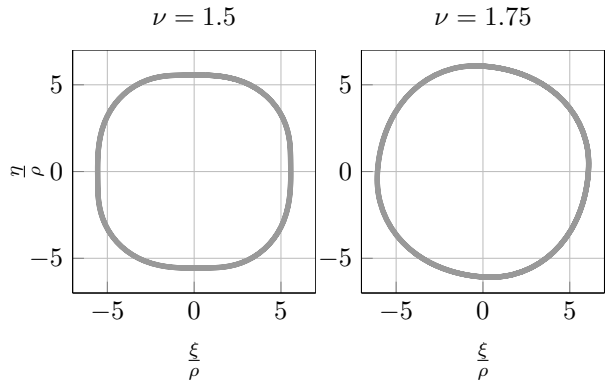

Figure 11. Limit cycle orbits for purely frictional internal damping and viscous external damping ($D_i = 0$, $\rho = 0.05$) at $\nu = 1.5$, $\nu = 1.75$.

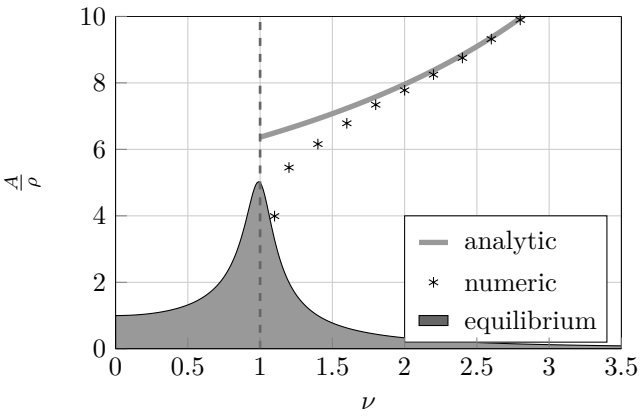

Figure 12. Equilibrium set $\mathcal{E}$, analytical approximation A_{LC} an numerical results of limit cycle amplitudes vs. ν for $D_e = 0.1$, $D_i = 0.02$, $r = 0.05$ (detail).

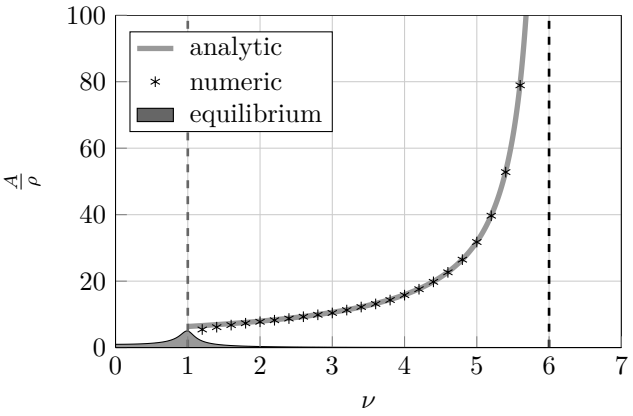

Figure 13. Equilibrium set $\mathcal{E}$, analytical approximation A_{LC} an numerical results of limit cycle amplitudes vs. ν for $D_e = 0.1$, $D_i = 0.02$, $r = 0.05$ (overview).

librium" refers to the co-rotating frame $\mathcal{R}$, an observer from the inertial system $\mathcal{I}$ will measure oscillations at rotor frequency ν and with a constant amplitude, which corresponds to the distance of the rest position within $\mathcal{E}$ from the origin O.

As the critical speed $\nu_{\mathrm{crit}} = 1$ is exceeded, the equilibrium set loses stability and the system state converges to an attractively stable limit cycle. For the present case of vanishing viscous internal damping, the limit cycle amplitude is constant for almost all speeds and only depends on ν near to the bifurcation point. This friction induced limit cycle excists for all supercritical speeds. For an inertial observer, this limit cycle will have the constant amplitude A_{LC} and the oscillations frequency ${}^{I}\omega_{\mathrm{LC}} = 1$.

2.3 Internal dissipation due to co-rotating friction and viscous damping

Considering internal viscous damping in addition to the co-rotating frictional dissipation limit cycle amplitudes are given by the full equation (14) and do only exist within the speed range $1 < \nu < 1 + \frac{D_e}{D_i}$, i.e. limit cycles will only exist between the resonance speed and the linear stability margin. The corresponding amplitudes are outlined examplarily for the parameter set $D_e = 0.1, D_i = 0.02, r = 0.05$ in figures 12 (details) and in figure 13 (overview). For these parameter values, the linear stability margin – and thus the upper limit of the existence intervall of A_{LC} is at $\nu = 3$. The oscillation frequency does not depend on D_i and thus corresponds to that found before, cf. figure 10.

As already found in sect. 2.2 for the case of only co-rotating frictional damping, a self-excited limit cycle appears at the critical speed $\nu = 1$. However, the limit cycle amplitude now is no longer constant over the rotor speed, but increases hyperbolically as it approaches the pole at $\nu = 1 + \frac{D_e}{D_i}$. Once this singularity has been trespassed, limit cycles due to internal friction do no longer exist and the amplitudes will be limited by some other nonlinearities, which are not contained within the model discussed here.

Obviously, the frictional part of the internal damping not only induces self-excited vibrations, but also strongly interacts with the viscous part of the internal damping. From a physical point of view, this seems reasonable according to the following line of reasoning: for the classical linear problem, the internal damping D_i may feed energy into the system and eventually lead to self-excited vibrations as the linear stability threshold $\nu_{\mathrm{crit}} = 1 + \frac{D_e}{D_i}$ is passed. Internal damping due to friction produces a self-excited limit cycle once the resonance speed $\nu = 1$ has been passed. As the rotational speed is increased, the internal viscous damping D_i will feed more and more energy per cycle into the system, thus leading to larger and larger limit cycle amplitudes. Within a certain range, the frictional dissipation and the external viscous damp-

ing are able to compensate the energy feed-in by the viscous internal damping. However, once the threshold of the linear stability problem has been trespassed, the viscous internal damping can no longer be compensated by neither the viscous external damping nor the frictional damping. By this, it is plausible that also for the problem comprising frictional and viscous internal damping, the stability margin of the linear problem still has a meaning.

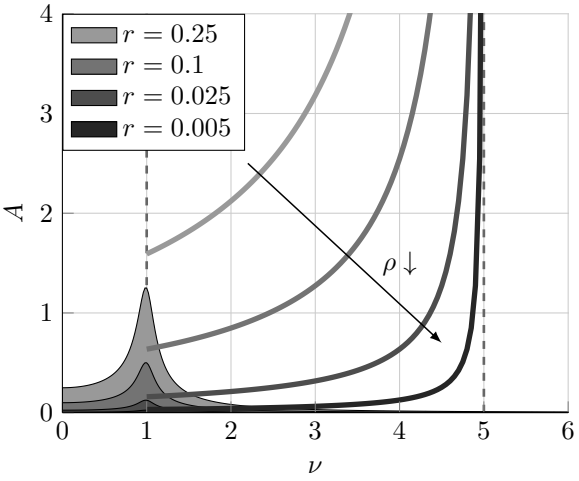

Figure 14. Oscillation amplitudes varying r and $D_e/D_i = 2$.

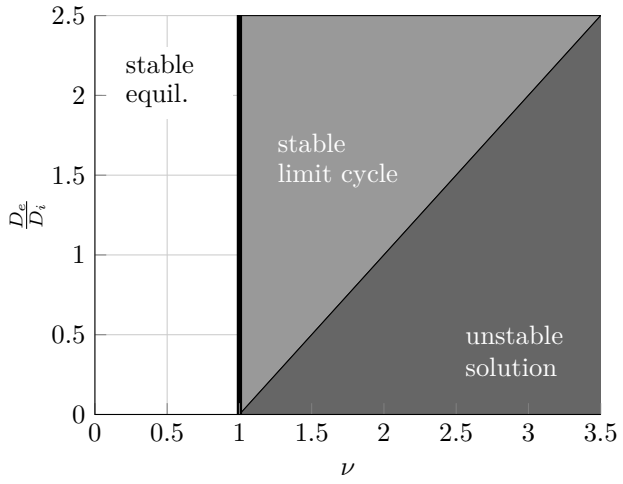

Figure 15. Enhanced stability chart accounting for internal viscous damping and as well as internal frictional damping.

3. CONCLUSIONS

Within this contribution the classical problem of self-excitation of elastic rotors due to co-rotating internal dissipation has been reviewed and extended in order to also account for non-viscous frictional forces contributing to the internal damping. To this purpose the classical Jeffcott rotor (Laval-rotor) model with viscous internal damping and viscous external damping has been extended by adding co-rotating dry friction forces. Numerical simulations indicated limit cycles for operational conditions above the critical speed. This observation has been proved by analytically approximations for sticking and sliding friction elements using Galerkin's method.

- Due to the set-valued character of stiction forces the unique steady state solution of the smooth problem turns into an entire set $\mathcal{E}$ of possible solutions for sticking friction elements. The size of this set behaves similar to the magnification function of a forced 1DoF-system and may become very large near the critial speet at $\nu = 1$.
- As long as the system rests at a sticking solution within $\mathcal{E}$ the external observer will measure oscillations of constant amplitude having the rotational frequency of the rotor. Based on frequency, such solutions could mistakenly be interpreted as unbalance excitation.
- For subcritical speeds $\nu < 1$ the set $\mathcal{E}$ is attractive and any initial condition will converge to this set. For supercritical speeds $\nu > 0$ the set $\mathcal{E}$ becomes unstable: although the system state may still remain in $\mathcal{E}$ (for sticking friction elements), small perturbations will lead to growing oscillations.
- As the rotor passes through $\nu = 1$ the internal frictional dissipation gives rise to a stable limit cycle. This limit cycle exists within the interval $1 < \nu < 1 + \frac{D_e}{D_i}$. An external observer will observe oscillatons at a frequencey ${}^I\omega_{\mathrm{LC}} = 1$. The corresponding orbit will be whirling backward with respect to the co-rotating frame of reference.
- Similar to viscous internal damping, frictional internal damping may destabilize the steady state solutions. However, in contrast to viscous damping this happens quite earlier at $\nu = 1$ and leads to finite limit-cycle amplitudes.
- As the rotation frequency ν approaches the linear stability margin $\nu_{\mathrm{crit}} = 1 + \frac{D_e}{D_i}$ the amplitude of the limit cycle grows hyperbolically. As this linear stability threshold is exceeded, the system investigated within this study is not able to predict a stationary solution anymore: the system state growths towards another nonlinear attractor.

Thus, it may be concluded that co-rotating frictional damping changes the stability and bifurcation behavior significantly. In particular, for systems with pronounced non-viscous frictional internal dissipation – as will be the case for most assembled rotors consisting of several parts with joints – the stability border ν_{crit} of the linear

system may give totally wrong threshold speeds for the occurence of self-excited vibrations.

Thus, for systems incorporating internal frictional dissipation it will rather be adequate to investigate the occurence as well as the amplitude of limit cycles. Consequently instead of the traditional discrimination between "stable" and "unstable" (as given by the linear analysis), one should rather ask whether vibrations occur and how relevant in terms of amplitude they will be for the operation of the system.

REFERENCES

[1] V.V. Bolotin and G. Herrmann. *Nonconservative problems of the theory of elastic stability*, volume 1991. Pergamon Press, 1963.

[2] A. Tondl. *Some problems of rotor dynamics*. Publishing House of the Czechoslovak Academy of Sciences, 1965.

[3] D. Childs and D.W. Childs. *Turbomachinery rotordynamics: phenomena, modeling, and analysis*. Wiley-Interscience, 1993.

[4] T. Yamamoto and Y. Ishida. *Linear and nonlinear rotordynamics: a modern treatment with applications*. Wiley-Interscience, 2001.

[5] A. Boyaci, H. Hetzler, W. Seemann, C. Proppe, and J. Wauer. Analytical bifurcation analysis of a rotor supported by floating ring bearings. *Nonlinear Dynamics*, 57(4):497–507, 2009.

[6] R. Gasch, R. Nordmann, and H. Pfützner. *Rotordynamik*. Springer, 2002.

[7] A. Muszynska. Rotor-To-Stationary Element Rub-Related Vibration Phenomena in Rotating Machinery–Literature Suryey. *Shock and Vibration Digest*, 21(3), 1989.

[8] W. Kellenberger. Erzwungene Biegeschwingungen einer anisotrop gelagerten Scheibenwelle mit Kreiselwirkung und Drehträgheit, äußerer und innerer Dämpfung. *Forschung im Ingenieurwesen*, 48(3):65–73, 1982.

[9] B.L. Newkirk. Measurement of internal friction in a revolving deflected shaft. *General Electric Review*, pages 554–558, 1925.

[10] A.L. Kimball. Internal friction theory of shaft whirling. *General Electric Review*, pages 244–251, 1924.

[11] F.F. Ehrich. Shaft whirl induced by rotor internal damping. *Journal of Applied Mechanics*, pages 279–282, 1964.

[12] Y. Ishida and T. Yamamoto. Forced oscillations of a rotating shaft with nonlinear spring characteristics and internal damping (1/2 order subharmonic oscillations and entrainment - in german). *Nonlinear Dynamics*, 4(5):413–431, 1993.

[13] J. Fischer and J. Strackeljan. Some considerations of modelling internal friction in rotor shaft connections. In *Proceedings of 12th World Congress in Mechanism and Machine Science IFToMM*, 2007.

[14] G. Siegl. *Das Biegeschwingungsverhalten von Rotoren, die mit Blechpaketen besetzt sind (Lateral Vibrations of Rotors with Laminar Stacks - in German)*. Dissertation thesis, TU Berlin, 1981.

[15] V. Luchscheider, K. Willner, and M. Maidorn. Development of a contact and a material model of laminated stacks. In *Electric Drives Production Conference (EDPC), 2013 3rd International*, pages 1–5. IEEE, 2013.

[16] V. Luchscheider. *Experimentelle und numerische Identifikation eines homogenisierten Materialmodells für Blechpakete elektrischer Maschinen (Experimental and numerical Identification of a homogenized Material Model for Metal Sheet Stacks of Electric Machinery)*. Dissertation thesis, University of Erlangen, 2016.

[17] JP Den Hartog. *Mechanical vibrations*. Dover Publications Inc.(Originally published: McGraw-Hill 1956), 1985.

[18] K Klotter. Theorie der reibschwingungsdämpfung. *Ingenieur Archiv*, 9:137–162, 1938.

[19] E. Marui and S. Kato. Forced vibration of a base-excited single-degree-of-freedom system with coulomb friction. *Journal of dynamic systems, measurement, and control*, 106:280, 1984.

[20] L. Gaul and J. Lenz. Nonlinear dynamics of structures assembled by bolted joints. *Acta Mechanica*, 125(1):169–181, 1997.

[21] A. Tondl. Quenching of self-excited vibrations: effect of dry friction. *Journal of Sound and Vibration*, 45(2):285–294, 1976.

[22] H. Yabuno, Y. Kunitho, T. Kashimura, et al. Analysis of the van der Pol System With Coulomb Friction Using the Method of Multiple Scales. *Journal of Vibration and Acoustics*, 130, 2008.

[23] H. Hetzler. On the effect of nonsmooth coulomb friction on hopf bifurcations in a 1-dof oscillator with self-excitation due to negative damping. *Nonlinear Dynamics*, pages 1–14, 2012.

[24] Hartmut Hetzler. On the effect of non-smooth coulomb damping on flutter-type self-excitation in a non-gyroscopic circulatory 2-dof-system. *Nonlinear Dynamics*, pages 1–19, 2013.

[25] Hartmut Hetzler. Bifurcations in autonomous mechanical systems under the influence of joint damping. *Journal of Sound and Vibration*, 333(23):5953–5969, 2014.

[26] H Yabuno, R Oowada, and N Aoshima. Effect of coulomb damping on buckling of a simply supported

beam. *Proc. of DETC99, Las Vegas, NV*, pages 1–12, 1999.

[27] R.I. Leine and N. van de Wouw. *Stability and convergence of mechanical systems with unilateral constraints*. Springer Verlag, 2008.